

SAMPLE DILUTION FOR AMS ^{14}C ANALYSIS OF SMALL SAMPLES (30–150 $\mu\text{g C}$)

M de Rooij¹ • J van der Plicht • H A J Meijer

Centre for Isotope Research (CIO), University of Groningen, the Netherlands.

ABSTRACT. We investigated sample dilution as a technique for accelerator mass spectrometry (AMS) radiocarbon analysis of very small samples (down to 30 μg). By diluting such samples up to a total weight of 200 μg , we can still perform reliable AMS measurements and improve the success rate significantly for targets that are difficult to measure. A disadvantage of this dilution technique is a loss of measurement precision. In addition, calculations of the $^{14}\text{C}/^{12}\text{C}$ isotope ratios and the uncertainties therein are not straightforward because of peculiarities in isotope fractionation processes in the AMS system. Therefore, to make sample dilution a routine method in our laboratory, we did extensive theoretical and experimental research to find the optimum conditions for all relevant parameters. Here, we report on the first detailed study dealing with all aspects of sample dilution. Our results can be applied in general. As an illustrative test case, we analyze ^{14}C data for CO_2 extracted from an ice core, from which samples of 35 $\mu\text{g C}$ or less are available.

INTRODUCTION

The development of the accelerator mass spectrometry (AMS) technique in the 1980s caused a tremendous increase in the application of radiocarbon. Worldwide, the number of ^{14}C analyses grew to tens of thousands annually. AMS offers undisputed advantages over the conventional, low-background counting technique. Much shorter analysis times are mainly responsible for the rapid growth in the number of analyses. At the Groningen ^{14}C laboratory, we measure a modern sample in 45 min using the accelerator, whereas our conventional technique takes 48 hr. In addition, the required sample amount is much smaller: a fraction of 1 mg C for AMS compared to 1–5 g of carbon for conventional dating. This created a wide range of extended and new ^{14}C applications, like dating of pollen and macrofossils in paleoecology (van Geel et al. 1998), dating of finds such as single-year grains (Bruins et al. 2003) and mummy hairs (van der Plicht et al. 2004) in archaeology, ^{14}C analysis of atmospheric CO_2 from just a few liters of air in atmospheric science (Meijer et al. 2006), and even ^{14}C dating of an ice core in glaciology (van de Wal et al. 2007), to mention just a few examples from our own laboratory.

In principle, the lower limit of the sample size required for AMS analysis is far below 1 mg C, because a modern sample of 1 mg C still contains about 6×10^7 ^{14}C atoms. Several AMS laboratories have been working on reduction of the required sample size down to 10–150 $\mu\text{g C}$, by optimizing the graphite production (Santos et al. 2007), experimenting with catalyst handling before and after the graphitization process (Klinedinst et al. 1994; Hua et al. 2004), or even by using alternative ion sources (Schneider et al. 2004; Uhl et al. 2005). The results of these efforts have been impressive, but 4 severe problems keep occurring:

1. Increased and more variable background levels;
2. Mass-dependent $^{14}\text{C}/^{12}\text{C}$ ratios, and thus normalization;
3. Lower precision of the ^{14}C measurement;
4. Considerable decrease in the success rate of measurements.

Problem (1) is caused by the smaller samples being more susceptible to contamination. A contaminant with a more or less constant mass increases the background levels for these samples, whereas accidental contamination causes stronger variability. We can partly correct for this background effect, but the mass-dependent background results in less accuracy. Problem (2) is possibly related to space charge effects in the ion source during sputtering (von Reden et al. 1998). It has also been

¹Corresponding author. Email: m.de.rooij@rug.nl.

associated with a combination of modern and dead contamination due to the preparation process, including the catalyst (Brown and Southon 1997; Santos et al. 2007). An accurate analysis can still be obtained, by using reference targets of the same size as the small samples. However, the increased number of reference targets in the batch reduces the measurement capacity. Another possibility is to use a mass- (or current-) dependent correction for the activity calculation of small samples (Alderliesten et al. 1998). Then, the phenomenon has to be reproducible. Problem (3) is connected to the first 2 problems along with the number of ^{14}C atoms counted in the detector. Increasing the target current and/or reducing the amount of catalyst might help to improve the sputter yield; however, because of the small sample amount, the increased sputter yield does not last throughout the entire sample measurement. This is one of the issues leading to problem (4). Producing a high-quality target that guarantees an accurate analysis for a small amount of sample material is a difficult task. Usually, a small sample is made from a limited amount of precious material. With no material remaining, failure to produce a successful ^{14}C analysis is highly unwanted.

To avoid these problems, using our HVEE 4130 ^{14}C AMS system (Gott dang et al. 1995), we decided to study sample dilution in detail. The direct occasion for this study was the accurate ^{14}C analysis of 18 small, precious ice-core samples. These samples were taken from the EDML ice core that was drilled in Dronning Maud Land (DML) as part of the European Project for Ice Coring in Antarctica (EPICA). We received the CO_2 extracted from the air bubbles of the ice core, which contained only 35 $\mu\text{g C}$. Therefore, we investigated the use of sample dilution for these samples.

After pretreatment and combustion of the small sample, we add a CO_2 gas with a known ^{14}C activity. This approach avoids the problems mentioned under (2) and (4), whereas the effects of problem (1) will be significantly lower. Considering problem (3), we will obviously pay a price regarding precision using sample dilution. However, the advantages of analyzing a normal-sized sample might well compensate for this. Achieving a high analysis success rate, with as high accuracy as possible, is the main motivation for our study.

In conventional laboratories, undersized samples are usually diluted with a ^{14}C -free CO_2 gas to the required amount of material (Mook and Streurman 1983). The ^{14}C activity of the original sample is found using a simple mass balance equation. For AMS, however, the AMS-induced isotope fractionation complicates the calculation of the small sample result. Our research questions are, therefore, summarized as follows:

1. How do we determine the normalized activity of the original (small) sample?
2. How do we determine the uncertainty in the normalized activity of the original sample?
3. What is the best choice for the diluent gas to achieve the best precision?
4. What is the smallest sample size that still yields accurate ^{14}C activities?
5. What is the background, and thus age limit, for a small sample analyzed by using sample dilution?

In the next section, we present 3 procedures to find the normalized activity. This includes a detailed analysis of the error propagation from the original error sources to the final uncertainty in the original sample result. Section 3 describes the experimental setup we used to verify these theoretical considerations in an extensive dilution experiment. We deliberately used larger sample masses for some of the sample series in the experiment. The results are discussed for: i) normal samples diluted to 2 mg C; ii) small samples diluted to 200 $\mu\text{g C}$; iii) 200- $\mu\text{g C}$ backgrounds that reveal the background values and thus the age limit for small samples; and iv) the normalized activity of the CO_2 extracted from the air bubbles of the 18 ice-core samples. Finally, we summarize our experiences with sample dilution, answer our research questions, and make suggestions for further work.

THEORETICAL BACKGROUND AND CALCULATION STUDY

After sample dilution, the AMS system measures the ¹⁴C activity of the total (diluted) sample. So, we need to calculate the normalized activity of the original (small) sample. This is not straightforward because of AMS-induced isotope fractionation. Just using a simple mass balance equation with the known activity of the diluent gas is not sufficient. We need to know the δ¹³C value that the AMS system would have measured for the original sample, if it had not been diluted. We present 3 related, but different, procedures to find this δ¹³C value and obtain a reliable result for the normalized activity of the original sample.

In our calculation, we first distinguish between the 5 activities shown in the upper half of Table 1. Only the AMS ¹⁴C activity of the total sample (¹⁴a_{tot}) is actually measured by the AMS system. ¹⁴a_{org} and ¹⁴a_{dil} represent the ¹⁴C activity that the AMS would have measured for the original sample and the diluent gas only, that is, if the sample had not been diluted. We calculate ¹⁴a_{org} from ¹⁴a_{tot}, using a mass balance equation:

$$^{14}a_{org} = \frac{^{14}a_{tot} - (x \cdot ^{14}a_{dil})}{1 - x} \tag{1}$$

where the dilution factor $x = m_{dil} / (m_{org} + m_{dil})$ is the ratio between the diluent gas and total sample mass. We find ¹⁴a_{dil} from ¹⁴a (the non-δ¹³C normalized activity of the diluent gas) and α_{AMS} (the ¹³C fractionation factor of the total graphitization process, including AMS analysis):

$$^{14}a_{dil} = \alpha_{AMS}^2 \cdot ^{14}a \tag{2}$$

Table 1 Upper half: the 5 activities we distinguish in our calculation. Only ¹⁴a_{tot} is actually measured by the AMS system. ¹⁴a_{org} and ¹⁴a_{dil} represent the ¹⁴C activity that the AMS would have measured for the original sample and the diluent gas only, i.e. if the sample had not been diluted. Lower half: the 5 δ¹³C values we distinguish in our procedures. Only δ¹³C_{tot} is actually measured by the AMS system. δ¹³C_{org} represents the δ¹³C value that the AMS would have measured for the original sample, if the sample had not been diluted. The true δ¹³C values can be measured by stable isotope ratio mass spectrometry (IRMS).

Sample	True ¹⁴ C activity non-normalized	AMS ¹⁴ C activity non-normalized	Calculated activity normalized
original (small)		¹⁴ a _{org}	¹⁴ a _{org,N}
diluent gas	¹⁴ a	¹⁴ a _{dil}	
total (diluted)		¹⁴ a _{tot}	
Sample	True δ ¹³ C value	AMS δ ¹³ C value	
original (small)	δ ¹³ C _{org,IRMS}	δ ¹³ C _{org}	
diluent gas	δ ¹³ C _{dil,IRMS}		
total (diluted)	δ ¹³ C _{tot,IRMS}	δ ¹³ C _{tot}	

If we dilute the sample with a reference material, ¹⁴a is accurately known. It results in ¹⁴a_{dil} = 0, if the diluent gas is ¹⁴C free. How to find α_{AMS} is explained below.

Then, we distinguish between the 5 δ¹³C values shown in the lower half of Table 1. Only δ¹³C_{tot} is measured by the AMS system. δ¹³C_{org} represents the δ¹³C value that the AMS would have measured

for the original sample, if the sample had not been diluted. The true $\delta^{13}\text{C}$ values can be measured by stable isotope ratio mass spectrometry (IRMS).

In order to find $\delta^{13}\text{C}_{\text{org}}$ we can use 3 different procedures (A, B, or C):

Procedure A: $\delta^{13}\text{C}_{\text{org,IRMS}}$ is measured by IRMS before the sample is diluted. In this case, $\delta^{13}\text{C}_{\text{org}}$ is found from:

$$\delta^{13}\text{C}_{\text{org}} = \alpha_{\text{AMS}} \cdot (1 + \delta^{13}\text{C}_{\text{org,IRMS}}) - 1 \quad (3)$$

When we measure $\delta^{13}\text{C}_{\text{dil,IRMS}}$ by IRMS as well, we can deduce α_{AMS} on a sample-to-sample basis:

$$\alpha_{\text{AMS}} = \frac{1 + \delta^{13}\text{C}_{\text{tot}}}{1 + (x \cdot \delta^{13}\text{C}_{\text{dil,IRMS}} + (1-x) \cdot \delta^{13}\text{C}_{\text{org,IRMS}})} \quad (4)$$

Procedure B: $\delta^{13}\text{C}_{\text{tot,IRMS}}$ is measured by IRMS after the sample is diluted.

This is usually done in case we cannot measure $\delta^{13}\text{C}_{\text{org,IRMS}}$ directly (e.g. if the dilution has already been done elsewhere or if we cannot afford to lose sample material for the $\delta^{13}\text{C}$ analysis). Following this procedure, $\delta^{13}\text{C}_{\text{org}}$ is found from:

$$\delta^{13}\text{C}_{\text{org}} = \alpha_{\text{AMS}} \cdot \left(1 + \frac{\delta^{13}\text{C}_{\text{tot,IRMS}} - (x \cdot \delta^{13}\text{C}_{\text{dil,IRMS}})}{1-x} \right) - 1 \quad (5)$$

Now, it is straightforward to deduce α_{AMS} on a sample-to-sample basis:

$$\alpha_{\text{AMS}} = \frac{1 + \delta^{13}\text{C}_{\text{tot}}}{1 + \delta^{13}\text{C}_{\text{tot,IRMS}}} \quad (6)$$

Procedure C: neither $\delta^{13}\text{C}_{\text{org,IRMS}}$ nor $\delta^{13}\text{C}_{\text{tot,IRMS}}$ can be measured by IRMS.

In this procedure, we assume α_{AMS} to be the same as for the total sample and the standards in the batch, which have the same size. We take the average of the ^{13}C fractionation factors for the standards, which is found from the standard's true $\delta^{13}\text{C}$ value and its AMS measured $\delta^{13}\text{C}$ value. In this case, $\delta^{13}\text{C}_{\text{org}}$ is found from:

$$\delta^{13}\text{C}_{\text{org}} = \alpha_{\text{AMS}} \cdot \left(1 + \frac{\left(\frac{1 + \delta^{13}\text{C}_{\text{tot}}}{\alpha_{\text{AMS}}} - 1 \right) - x \cdot \delta^{13}\text{C}_{\text{dil,IRMS}}}{1-x} \right) - 1 \quad (7)$$

Usually, this value for α_{AMS} is very close to unity (the AMS $\delta^{13}\text{C}$ results are usually calibrated using these standards), but it might vary from sample to sample. Therefore, procedures A and B are preferred over C to find the $\delta^{13}\text{C}_{\text{org}}$ values and α_{AMS} .

Following one of these procedures, we can find the normalized activity of the original sample (represented by $^{14}\text{a}_{\text{org,N}}$) as if it had been analyzed in its pure, undiluted form. With the $\delta^{13}\text{C}_{\text{org}}$ value, we normalize $^{14}\text{a}_{\text{org}}$ to $\delta^{13}\text{C} = -25\text{‰}$:

$$^{14}a_{org,N} = ^{14}a_{org} \left(\frac{0.975}{1 + \delta^{13}\text{C}_{org}} \right)^2 \quad (8)$$

In case we would like to know the age of the original sample, it can be calculated from:

$$age = -\ln(^{14}a_{org,N}) \cdot 8033 \quad (9)$$

using the conventional half-life of 5568 yr (Mook and Streurman 1983).

It is of crucial importance to obtain a good estimate for the standard deviation in $^{14}a_{org,N}$. To do that, $^{14}a_{org,N}$ is first expressed as a function of independent variables by proper substitution of the equations above. It is then straightforward to find the standard deviation in $^{14}a_{org,N}$ ($\sigma[^{14}a_{org,N}]$) from the partial derivatives of $^{14}a_{org,N}$ with respect to variable x_i ($\partial^{14}a_{org,N}/\partial x_i$) and the error in the variable ($\sigma[x_i]$):

$$\sigma[^{14}a_{org,N}] = \left[\left(\frac{\partial^{14}a_{org,N}}{\partial x_1} \cdot \sigma[x_1] \right)^2 + \left(\frac{\partial^{14}a_{org,N}}{\partial x_2} \cdot \sigma[x_2] \right)^2 + \dots + \left(\frac{\partial^{14}a_{org,N}}{\partial x_i} \cdot \sigma[x_i] \right)^2 \right]^{1/2} \quad (10)$$

The standard deviation in the activity of the original sample $\sigma[^{14}a_{org}]$ is found in a similar way.

To determine the size of the standard deviations and find the optimum diluent gas, we studied the behavior of $\sigma[^{14}a_{org}]$ and $\sigma[^{14}a_{org,N}]$ in detail. We calculated the terms in $\sigma[^{14}a_{org}]$ and $\sigma[^{14}a_{org,N}]$ according to the 3 procedures, for both small- and normal-sized samples. In the calculation study, we varied the values for the variables of the original sample ($^{14}a_{org} \in [0, 100\%]$, $\delta^{13}\text{C}_{org,IRMS} \in [-30, 0\%]$) and the diluent gas ($^{14}a_{dil} \in [0, 100\%]$, $\delta^{13}\text{C}_{dil,IRMS} \in [-40, +10\%]$), covering the full range of datable materials. The original sample and diluent gas mass were also varied: $m_{dil} = 200 - m_{org}$ with $m_{org} \in [20 \text{ to } 180 \mu\text{g C}]$ for small samples and $m_{dil} = 2 - m_{org}$ with $m_{org} \in [0.2 \text{ to } 1.8 \text{ mg C}]$ for normal-sized samples. We calculated $^{14}a_{tot}$, $\delta^{13}\text{C}_{tot,IRMS}$, and $\delta^{13}\text{C}_{tot}$ as a function of these variables assuming $\alpha_{AMS} = 0.9999$.

To make these calculations useful, we need to choose the errors of the independent variables carefully. To find realistic results, we determined these errors from the data we obtained during the last 6 yr of our long-standing experience with AMS ^{14}C dating (see Table 2). The error values differ for small- and normal-sized samples. Some of the numbers are relatively easy to establish, e.g. for m_{org} and $\delta^{13}\text{C}_{dil,IRMS}$. Others (like $^{14}a_{tot}$, ^{14}a , and $\delta^{13}\text{C}_{tot}$) require some more effort. To give an example: for normal-sized samples, $\sigma[^{14}a_{tot}]$ is based on general standard deviation behavior of samples with a mass $>0.7 \text{ mg C}$ (see Figure 1). The black dots are averages over many analyses over the years, and the open squares are the results for the standard deviations of our backgrounds and IAEA-C7, IAEA-C8, and HOxII standards during the past 6 yr. The fit that we use as parameterization, contains 3 terms: the spread in the background values, the Poisson statistics, and the spread in the standards.

We calculated $\sigma[^{14}a_{org}]$, $\sigma[^{14}a_{org,N}]$, and the individual terms in these standard deviations for all possible combinations of the variable values. Figure 2a shows $\sigma[^{14}a_{org}]$ and the 6 terms as a function of x for an original small sample ($^{14}a_{org} = 60\%$ and $\delta^{13}\text{C}_{org,IRMS} = -25\%$) diluted ($^{14}a_{dil} = 10\%$ and $\delta^{13}\text{C}_{dil,IRMS} = -5\%$) to $200 \mu\text{g C}$, using procedure B. The dominant term comes from the error in the AMS-measured ^{14}C activity of the total sample ($\sigma[^{14}a_{tot}]$). The $\sigma[\delta^{13}\text{C}_{tot,IRMS}]$ and $\sigma[\delta^{13}\text{C}_{tot}]$ terms are negligible compared to the others. Notice that the results for $\sigma[m_{org}]$ and $\sigma[m_{dil}]$ are identical. If the ^{14}C activity of the original sample is lower, e.g. $^{14}a_{org} = 20\%$, we find a similar result (see Figure 2b), except for the mass-related error contributions, $\sigma[m_{org}]$ and $\sigma[m_{dil}]$, which can also be neglected in this case.

Table 2 Overview of the variables to calculate $^{14}\text{a}_{\text{org}}$, $\sigma[^{14}\text{a}_{\text{org}}]$, $^{14}\text{a}_{\text{org,N}}$, and $\sigma[^{14}\text{a}_{\text{org,N}}]$, according to the 3 procedures. The error values are based on the data that we found during the last 6 yr of our long-standing experience with AMS ^{14}C dating. They differ for small- and normal-sized samples.

Variable x_i	Procedure(s) $^{14}\text{a}_{\text{org}}$	Procedure(s) $^{14}\text{a}_{\text{org,N}}$	Error in variable	
			$\sigma[x_i]$ Small samples	$\sigma[x_i]$ Normal-sized samples
m_{org}	A, B & C	A, B & C	$\sigma[m_{\text{org}}] = 0.01 * m_{\text{org}}$	$\sigma[m_{\text{org}}] = 0.001 * m_{\text{org}}$
m_{dil}	A, B & C	A, B & C	$\sigma[m_{\text{dil}}] = 0.01 * m_{\text{dil}}$	$\sigma[m_{\text{dil}}] = 0.001 * m_{\text{dil}}$
^{14}a	A, B & C	A, B & C	$\sigma[^{14}\text{a}] = \text{AMS based}$	$\sigma[^{14}\text{a}] = \text{AMS based}$
$^{14}\text{a}_{\text{tot}}$	A, B & C	A, B & C	$\sigma[^{14}\text{a}_{\text{tot}}] = \text{AMS based}$	$\sigma[^{14}\text{a}_{\text{tot}}] = \text{AMS based}$
$\delta^{13}\text{C}_{\text{tot}}$	A & B	A, B & C	$\sigma[\delta^{13}\text{C}_{\text{tot}}] = \text{AMS based}$	$\sigma[\delta^{13}\text{C}_{\text{tot}}] = \text{AMS based}$
$\delta^{13}\text{C}_{\text{dil,IRMS}}$	A	A, B & C	$\sigma[\delta\text{C}_{\text{dil,IRMS}}] = 0.2\text{‰}$	$\sigma[\delta\text{C}_{\text{dil,IRMS}}] = 0.03\text{‰}$
$\delta^{13}\text{C}_{\text{org,IRMS}}$	A	A	$\sigma[\delta\text{C}_{\text{org,IRMS}}] = 0.2\text{‰}$	$\sigma[\delta\text{C}_{\text{org,IRMS}}] = 0.03\text{‰}$
$\delta^{13}\text{C}_{\text{tot,IRMS}}$	B	B	$\sigma[\delta\text{C}_{\text{tot,IRMS}}] = 0.2\text{‰}$	$\sigma[\delta\text{C}_{\text{tot,IRMS}}] = 0.03\text{‰}$
α_{AMS}	C	C	$\sigma[\alpha_{\text{AMS}}] = 0.002$	$\sigma[\alpha_{\text{AMS}}] = 0.0009$

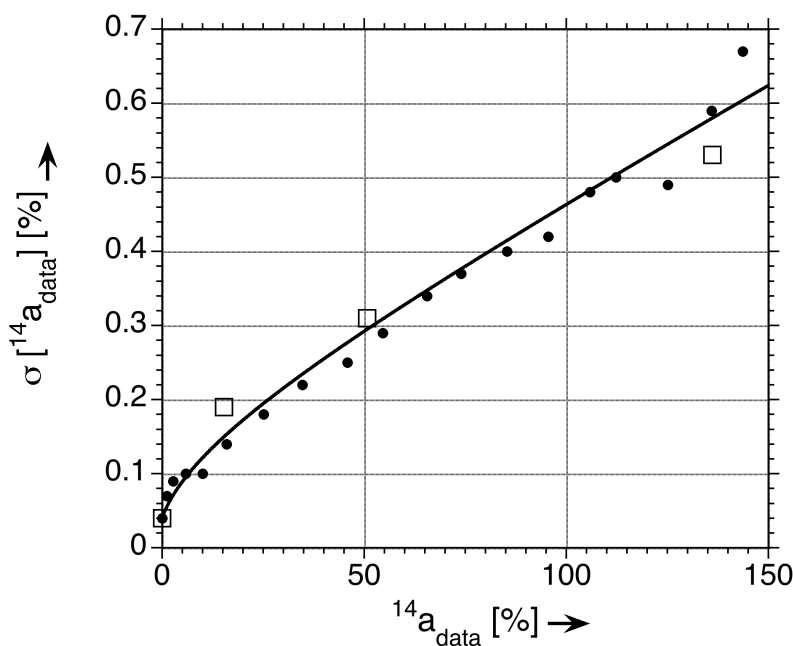


Figure 1 General behavior of the standard deviation ($\sigma[^{14}\text{a}_{\text{data}}]$) as a function of the non-normalized activity ($^{14}\text{a}_{\text{data}}$) for samples >0.7 mg C. The black dots are averages of calculated errors for many regular analyses over the years, and the open squares are the true standard deviations of our backgrounds and IAEA-C7, IAEA-C8, and HOxII standards over the last 6 yr. We use the fit as a parameterization for $\sigma[^{14}\text{a}_{\text{tot}}]$. It contains 3 terms: the spread in the background values, the Poisson statistics, and the spread in the standards.

Next, we investigated the difference between the ^{14}C activity of the original sample and the diluent gas. Figure 3a shows $\sigma[^{14}\text{a}_{\text{org}}]$ and the 6 terms as a function of $^{14}\text{a}_{\text{dil}}$ for an original small sample ($^{14}\text{a}_{\text{org}} = 20\%$ and $\delta^{13}\text{C}_{\text{org,IRMS}} = -25\text{‰}$) diluted ($\delta^{13}\text{C}_{\text{dil,IRMS}} = -5\text{‰}$, $x = 0.5$) to 200 μg C, according to procedure B. If $^{14}\text{a}_{\text{dil}} = ^{14}\text{a}_{\text{org}} = 20\%$, the $\sigma[m_{\text{org}}]$ and $\sigma[m_{\text{dil}}]$ terms are equal to zero. The masses do not contribute to the error if both activities are equal, but they increase linearly with the difference between $^{14}\text{a}_{\text{dil}}$ and $^{14}\text{a}_{\text{org}}$. Figure 3b shows the results if $^{14}\text{a}_{\text{org}} = 60\%$.

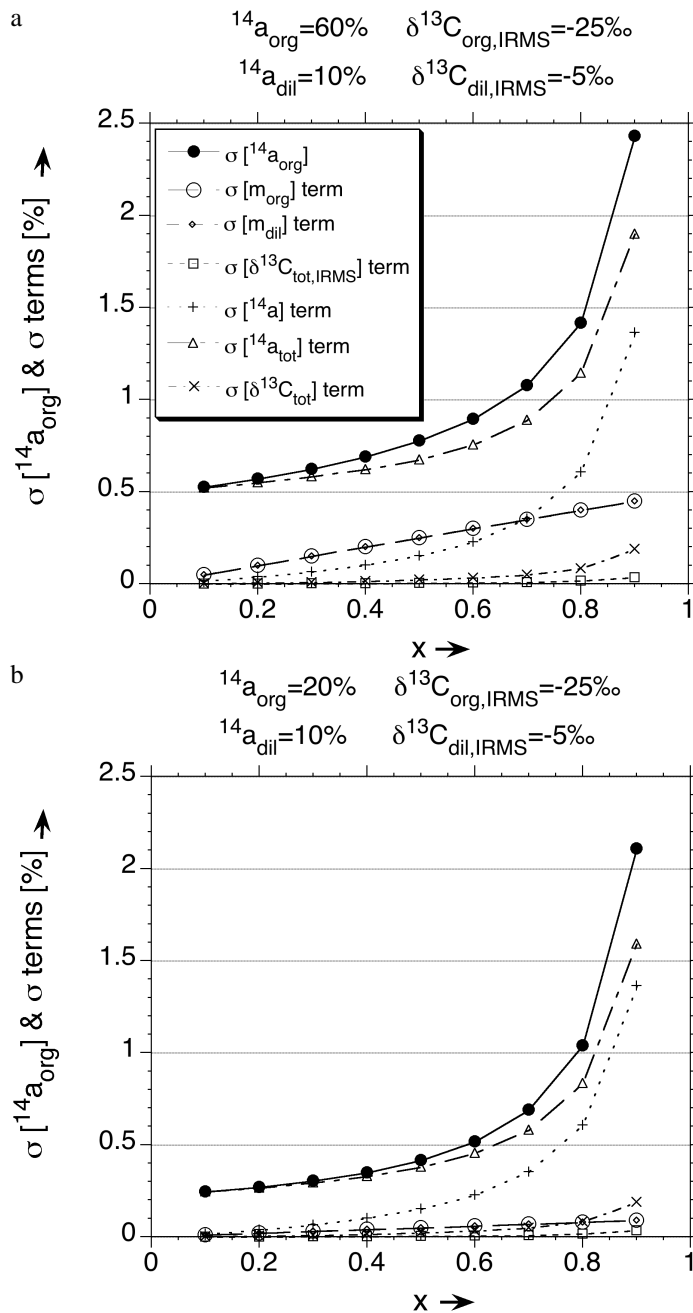


Figure 2 Results for $\sigma[^{14}\text{a}_{\text{org}}]$ and the 6 terms in $\sigma[^{14}\text{a}_{\text{org}}]$ as a function of x , calculated for an original sample ($\delta^{13}\text{C}_{\text{org,IRMS}} = -25\text{‰}$) diluted ($^{14}\text{a}_{\text{dil}} = 10\%$ and $\delta^{13}\text{C}_{\text{dil,IRMS}} = -5\text{‰}$) to $200\ \mu\text{g C}$, according to procedure B. a) For $^{14}\text{a}_{\text{org}} = 60\%$ and b) $^{14}\text{a}_{\text{org}} = 20\%$. Notice that the $\sigma[\text{m}_{\text{org}}]$ and $\sigma[\text{m}_{\text{dil}}]$ terms overlap.

Our calculation study shows that for the error propagation, all the $\sigma[\delta^{13}\text{C}]$ terms in $\sigma[^{14}\text{a}_{\text{org}}]$ can be neglected. For procedure C, $\sigma[^{14}\text{a}_{\text{org}}]$ contains a $\sigma[\alpha_{\text{AMS}}]$ term instead of the $\sigma[\delta^{13}\text{C}_{\text{tot}}]$ terms for procedures A and B. However, the contribution of this term is negligible too. The remaining terms can

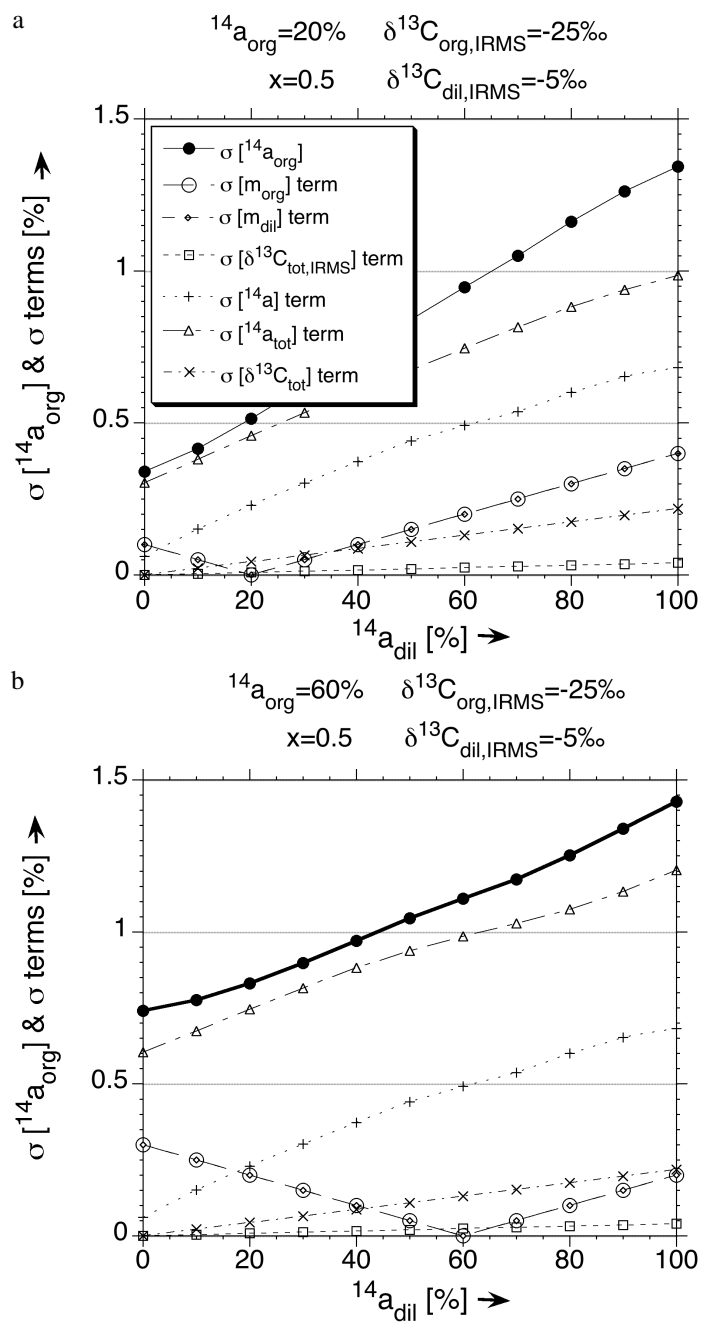


Figure 3 Results for $\sigma[^{14}\text{a}_{\text{org}}]$ and the 6 terms in $\sigma[^{14}\text{a}_{\text{org}}]$ as a function of $^{14}\text{a}_{\text{dil}}$, calculated for an original sample ($\delta^{13}\text{C}_{\text{org,IRMS}} = -25\text{‰}$) diluted ($\delta^{13}\text{C}_{\text{dil,IRMS}} = -5\text{‰}$ and $x = 0.5$) to $200 \mu\text{g C}$, according to procedure B. a) For $^{14}\text{a}_{\text{org}} = 20\%$ and b) for $^{14}\text{a}_{\text{org}} = 60\%$. Notice that the $\sigma[m_{\text{org}}]$ and $\sigma[m_{\text{dil}}]$ terms overlap.

be simplified substantially by neglecting the $\delta^{13}\text{C}$ -related parts and using $\alpha_{\text{AMS}} \approx 1$. We find that $\sigma[^{14}\text{a}_{\text{org}}]$ is, to a good approximation, the same for the 3 procedures. It is given by:

$$\sigma[{}^{14}a_{org,N}] \approx \left[\left(\frac{1}{1-x} \cdot \sigma[{}^{14}a_{tot}] \right)^2 + \left(\frac{-x}{1-x} \cdot \sigma[{}^{14}a] \right)^2 + \left(\frac{-x}{1-x} \cdot \frac{{}^{14}a_{tot} - {}^{14}a}{m_{org}} \cdot \sigma[m_{org}] \right)^2 + \left(\frac{{}^{14}a_{tot} - {}^{14}a}{m_{org}} \cdot \sigma[m_{dil}] \right)^2 \right]^{1/2} \tag{11}$$

The 1st term on the right-hand side comprises $\sigma[{}^{14}a_{tot}]$, which is the standard deviation in the AMS-measured ¹⁴C activity of the total sample. This term is always the largest. The 2nd term consists of the standard deviation in the non-normalized activity of the diluent gas ($\sigma[{}^{14}a]$). For a small mass ($x < 0.4$) and low activity of the diluent gas, it is almost negligible compared to the 1st term. However, it becomes relatively more important as x and ¹⁴a_{dil} increase (see Figures 2a and 3a). Mainly because of these first 2 terms that both depend on $1/(1-x)$, $\sigma[{}^{14}a_{org}]$ increases rapidly with x . The added amount of diluent gas should, therefore, be kept as small as possible to obtain a higher precision when using sample dilution. This is no surprise, of course.

The 3rd and 4th terms are the contributions of the error in the mass of the original sample ($\sigma[m_{org}]$) and diluent gas ($\sigma[m_{dil}]$), respectively. The terms are exactly the same in Figures 2 and 3 because $x/(1-x) = m_{dil}/m_{org}$ and we estimated $\sigma[m_{org}] = 0.001 \times m_{org}$ and $\sigma[m_{dil}] = 0.001 \times m_{dil}$. These terms also increase with x , so again the added diluent gas amount should be kept as small as possible. Indeed, the last 2 terms become more important if the difference between the activity of the original sample and diluent gas is larger. They might even become larger than the second term, especially when x and ¹⁴a_{dil} are small (see also Figures 2a and 3b). If we would choose the activity of the diluent gas to be equal to the activity of the original sample (¹⁴a_{tot} - ¹⁴a = 0), the last 2 terms would vanish. At first sight, this seems to make it worthwhile to guess the ¹⁴C activity of the original sample and use a diluent gas with a similar ¹⁴C activity. The above, however, gives the false impression that using a non-zero diluent gas may lead to a lower final uncertainty. One has to realize, namely, that both $\sigma[{}^{14}a_{tot}]$ and $\sigma[{}^{14}a]$ increase in absolute terms with the activity of the diluent gas, because a higher ¹⁴a_{dil} will also cause the activity of the total sample to be higher (see Figures 3a,b). Since the first term in (11) remains the most dominant one under all practical circumstances, $\sigma[{}^{14}a_{tot}]$ will increase with ¹⁴a_{dil}. So, to obtain a higher precision when using sample dilution, the diluent gas should be ¹⁴C free, a result that agrees with the common dilution practice so far. (But prior to this work, it was unclear to us whether this “common practice” was based on solid calculations or just on intuition or ease of use.) The choice for $\delta^{13}C_{dil,IRMS}$ is unimportant because the error terms containing $\delta^{13}C$ are negligible.

The standard deviation in ¹⁴a_{org,N} is very similar to $\sigma[{}^{14}a_{org}]$. To a good approximation, this is given by:

$$\sigma[{}^{14}a_{org,N}] = {}^{14}a_{org} \left[\left(\frac{\sigma[{}^{14}a_{org}]}{{}^{14}a_{org}} \right)^2 + (-2 \cdot \sigma[\delta^{13}C_{tot}])^2 \right]^{1/2} \tag{12}$$

for procedures A and B, and by:

$$\sigma[{}^{14}a_{org,N}] = {}^{14}a_{org} \left[\left(\frac{\sigma[{}^{14}a_{org}]}{{}^{14}a_{org}} \right)^2 + \left(\frac{-2}{1-x} \cdot \sigma[\delta^{13}C_{tot}] \right)^2 \right]^{1/2} \tag{13}$$

for procedure C.

In the latter case, the standard deviation in the normalized activity of the original sample will be larger. This is due to the second term in (13), which increases rapidly with x . Therefore, procedures A or B are again preferred over C because it will result in a higher precision for $^{14}\text{a}_{\text{org},N}$.

The calculation of the standard deviation in the conventional ^{14}C age of the original sample is equivalent to that for normal samples (Mook and Streurman 1983). For young samples, i.e. when $\sigma[^{14}\text{a}_{\text{org},N}]$ is small compared to $^{14}\text{a}_{\text{org},N}$, it is:

$$\sigma[\text{age}] = -8033 \cdot \frac{\sigma[^{14}\text{a}_{\text{org},N}]}{^{14}\text{a}_{\text{org},N}} \quad (14)$$

For older samples, the standard deviation in the sample age is calculated from the activities $^{14}\text{a}_{\text{org},N} + \sigma[^{14}\text{a}_{\text{org},N}]$ and $^{14}\text{a}_{\text{org},N} - \sigma[^{14}\text{a}_{\text{org},N}]$:

$$\sigma[\text{age}] = -8033 \cdot \ln\left(1 \pm \frac{\sigma[^{14}\text{a}_{\text{org},N}]}{^{14}\text{a}_{\text{org},N}}\right) \quad (15)$$

EXPERIMENTAL METHOD

To check our approximation for the standard deviation in $^{14}\text{a}_{\text{org},N}$ and our error values, we performed a series of dilution experiments. We used a variety of sample materials, with various values for ^{14}C activities and $\delta^{13}\text{C}$ (see Table 3). Hoekloos (HL) and Rommenhöller (RH) are ^{14}C -free natural CO_2 gases obtained from commercial suppliers. IAEA-C5 (wood) and IAEA-C7 (oxalic acid), which was developed by the Groningen Laboratory (Le Clercq et al. 1998), are distributed by the IAEA. VIRI-H is a whalebone sample, used for the Fifth International Radiocarbon Intercomparison (Scott et al. 2003). Sample 1 is a large sample of wood submitted to the Groningen Conventional Laboratory. Sample 2 is a large CO_2 sample of unknown origin.

Table 3 The ^{14}C activities and $\delta^{13}\text{C}$ values of materials we used in our dilution experiments. They are the averages of multiple analyses by AMS (^{14}C) and IRMS (^{13}C). The ^{14}C activities ($^{14}\text{a}_N$) are normalized for fractionation to $\delta^{13}\text{C} = -25\text{‰}$ and given in %. The $\delta^{13}\text{C}$ values are given in ‰ relative to the VPDB standard.

Material	Code	$^{14}\text{a}_N$ (%)	$\delta^{13}\text{C}$ (‰)
Hoekloos	HL	0 ± 0.07	-36.8 ± 0.03
Rommenhöller	RH	0 ± 0.04	-3.01 ± 0.03
IAEA-C5	C5	23.15 ± 0.11	-24.88 ± 0.04
IAEA-C7	C7	49.57 ± 0.19	-14.26 ± 0.02
VIRI-H	VH	30.42 ± 0.23	-16.35 ± 0.03
Sample 1	S1	54.71 ± 0.14	-25.63 ± 0.03
Sample 2	S2	42.59 ± 0.15	-25.66 ± 0.04

All materials, except HL and RH, were pretreated and combusted in large quantities to CO_2 by the Groningen Conventional Laboratory. Subsequently, they were used in small amounts by the Groningen AMS Laboratory for the dilution experiment. The ^{14}C activities and $\delta^{13}\text{C}$ values shown in Table 3 are the averages of multiple analyses by AMS (^{14}C) and IRMS (^{13}C). Their values do not differ significantly from the consensus values (C5 and C7) and the reported values (VH, S1, S2) from the Groningen Conventional Laboratory.

We prepared 6 series of 9 diluted samples, in triplicate. For the “unknown” original sample, we chose VH, VH, VH, S1, S1 and C7, respectively, with masses ranging from 0.2 to 1.8 mg C. They were diluted with RH, C5, S2, RH, C7, and RH, respectively, to a total sample size of 2 mg C (≈ 4 mL CO_2). Thus, the dilution factor x varied between 0.1 and 0.9. Next to these normal-sized samples, we prepared 1 series of 40 small C7 samples, with masses ranging from 15 to 145 μg C. All of them were diluted with HL to a total sample size of approximately 200 μg C (≈ 0.4 mL CO_2), with dilution factor x varying between 0.15 and 0.95. The $\delta^{13}\text{C}$ values of the original sample materials were measured by IRMS.

To prepare the 2-mg C samples, we used a glass vacuum system (see Figure 4). The approximate amount of CO_2 for the original sample was expanded from a cylinder over the main line (A) and the measurement volume (E). The pressure was adjusted by moving the piston in the variable volume (D) and accurately measured by a MKS Baratron[®] Type 626A absolute pressure transducer (F) after isolating the measurement volume by closing the surrounding valves. We waited for the pressure to stabilize under constant temperature conditions. The amount of CO_2 in the measurement volume was transferred to the mixing volume (B) using liquid nitrogen. There we added the diluent gas material following the same procedure. We took great care in thoroughly mixing the original sample and diluent gas before the total sample was expanded into the 3 sample bottles (C).

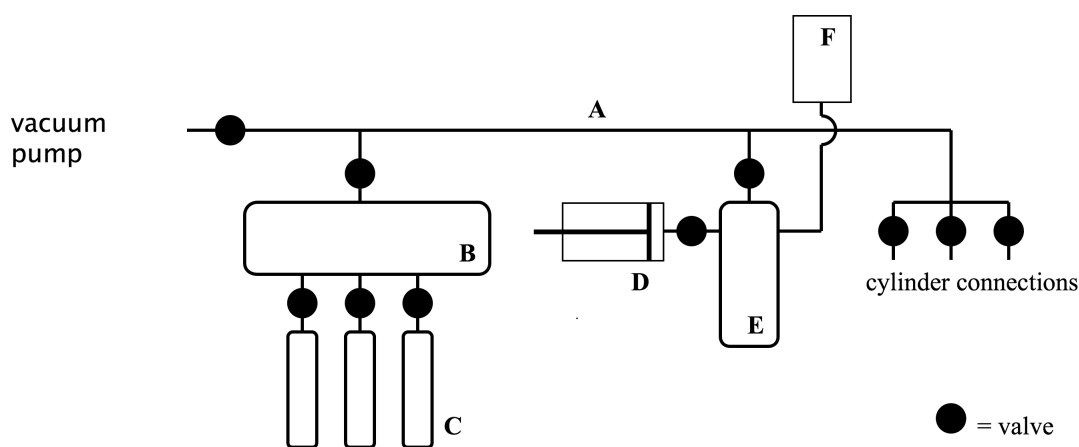


Figure 4 The glass vacuum system in which the diluted samples were prepared. It consists of a main line (A), mixing volume (B), sample bottles (C), piston in a variable volume (D), measurement volume (E), and pressure transducer (F).

The 200- μg C samples were prepared in a comparable setup following a similar procedure. Instead of a triplicate, however, we made only 1 specimen of each small sample.

First, the $\delta^{13}\text{C}$ value of the total sample was measured by IRMS for all samples but 10 of the 200- μg C samples. This way, we could check if the extra handling and IRMS measurement would contaminate the 200- μg C sample. Then, the CO_2 of all the samples was reduced to graphite with a H_2 excess ($\text{H}_2:\text{CO}_2 = 2.5:1$) at 600 $^\circ\text{C}$, using spherical Fe powder (1.5 mg, <325 mesh, 99.5% pure) as a catalyst (Aerts-Bijma et al. 1997). The graphite was pressed into 1.5-mm target holders, suitable for the ion source, with a small amount of Ag powder.

The Groningen ^{14}C AMS system simultaneously measures the $^{14}\text{C}/^{12}\text{C}$ and $^{13}\text{C}/^{12}\text{C}$ ratios of the total sample (van der Plicht et al. 2000). The 2-mg C and 200- μg C samples were measured in different batches with RH backgrounds and HOxII standards of the same size. For the 2-mg C samples, the

Cs temperature is set to 90 °C, and for the 200-µg C samples it was raised by 2–3 °C, to optimize the ^{13}C current during the measurement. Most batches containing the 2-mg C samples were measured in duplicate, directly after the first measurement was finished. (The batches containing the S1 and C7 samples diluted with RH were measured only once.) The $^{14}\text{C}/^{12}\text{C}$ ratios of the total sample and background samples are reported relative to the HOxII standard and normalized for fractionation to $\delta^{13}\text{C} = -25\text{‰}$ (Mook and van der Plicht 1999).

The normalized activity $^{14}a_N$ is calculated as follows:

$$^{14}a_N = 134.06 \cdot \frac{(^{14}\text{C}/^{12}\text{C})_{\text{sample}} - (^{14}\text{C}/^{12}\text{C})_{\text{bg}}}{(^{14}\text{C}/^{12}\text{C})_{\text{ref}} - (^{14}\text{C}/^{12}\text{C})_{\text{bg}}} \cdot \frac{\left(\frac{0.975}{1 + \delta^{13}\text{C}_{\text{sample}}}\right)^2}{\left(\frac{0.975}{1 - 0.0177}\right)^2} \quad (16)$$

where $^{14}\text{C}/^{12}\text{C}$ is the ratio of the number of ^{14}C moles and ^{12}C moles that are detected for the sample, the batch mean background (bg), and the batch mean HOxII standard (ref). The normalized activity and the $\delta^{13}\text{C}$ for the HOxII standard are 134.06% and -17.7‰ , respectively. The $^{13}\text{C}/^{12}\text{C}$ ratios for the sample and the HOxII standard are also used to calculate the $\delta^{13}\text{C}$ value:

$$\delta^{13}\text{C}_{\text{sample}} = \frac{(^{13}\text{C}/^{12}\text{C})_{\text{sample}}}{(^{13}\text{C}/^{12}\text{C})_{\text{ref}}} \cdot (1 - 0.0177) - 1 \quad (17)$$

where $(^{13}\text{C}/^{12}\text{C})_{\text{sample}}$ is the ratio for the sample and $(^{13}\text{C}/^{12}\text{C})_{\text{ref}}$ is the mean ratio for the HOxII standards in the batch.

However, to calculate the normalized activity of the original sample we used the non-normalized activity that was measured by AMS.

EXPERIMENTAL RESULTS AND DISCUSSION

Normal-Sized Samples Diluted to 2 mg C

The ^{14}C activity of the total sample ($^{14}a_{\text{tot}}$) was measured by the AMS system for the 6 sample series of 2 mg C. Figure 5 shows the non-normalized results for the 3 series of VH samples as a function of x . The series were diluted with RH, C5, and S2, respectively. Notice that the sample triplicates and their measurement duplicates are displayed just left and right of their x values. For the VH samples diluted with S2, $^{14}a_{\text{tot}}$ increases linearly with x because the ^{14}C activity of S2 is higher than the activity of VH. This also causes the standard deviation in the measured activity ($\sigma[^{14}a_{\text{tot}}]$) to increase in absolute terms with x for this series. The ^{14}C activity of C5 is slightly lower than that of VH, and RH is a ^{14}C -free gas.

We calculated the normalized activity for all the original samples ($^{14}a_{\text{org,N}}$) according to the 3 procedures, thereby obtaining 3 results for each of the sample triplicates and their measurement duplicates. They show excellent agreement with the ^{14}C activities in Table 3. See, for example, $^{14}a_{\text{org,N}}$ as a function of x , for the series of VH diluted with C5 (Figure 6a). Clearly, the spread in the results is larger for the larger x values. This is what we expect since the standard deviation in the normalized activity of the original sample ($\sigma[^{14}a_{\text{org,N}}]$) increases with x . It resembles the increase of $\sigma[^{14}a_{\text{org}}]$ with x that we found from the calculation study (see Figures 2a,b). In Figure 6a, we use the approximation for $\sigma[^{14}a_{\text{org,N}}]$ that we calculated with (11) and either (12) or (13), depending on the procedure. For the series of VH diluted with RH, these values are much smaller (Figure 6b). This is

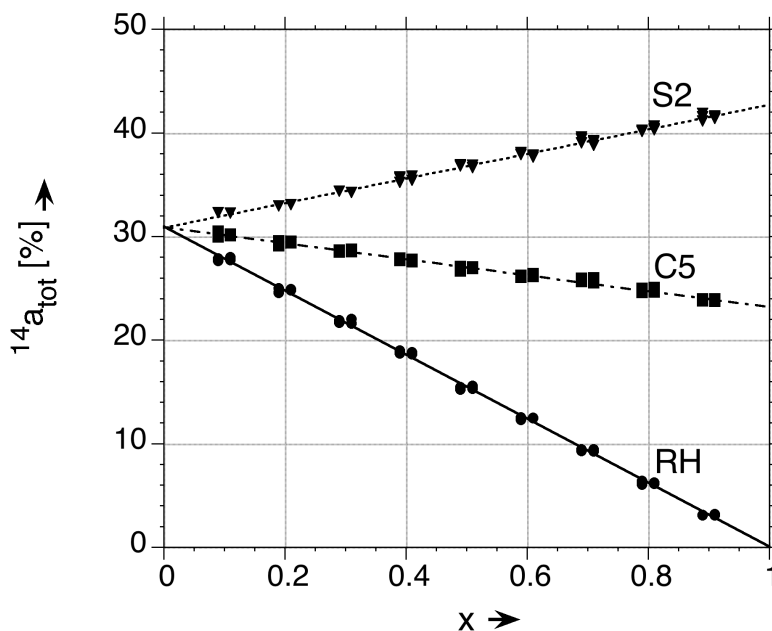


Figure 5 Measurement results for the 3 series of VH samples diluted to 2 mg C, showing the measured activity (non-normalized) of the total sample ($^{14}\text{a}_{\text{tot}}$) as a function of x . Standard deviations are not visible because they are smaller than the symbol size. Notice that the measurement duplicates (both in triplicate) are displayed just left and right of their x values.

mainly because the 1st term in (11), which is smaller for a lower diluent gas activity, is the dominant term. Even though the 3rd and 4th terms are smaller for the series diluted with C5, because in that case $^{14}\text{a}_{\text{tot}} - ^{14}\text{a} \approx 0$. The calculation study also showed that $\sigma[^{14}\text{a}_{\text{org}}]$ increases with $^{14}\text{a}_{\text{dil}}$ (Figures 3a,b). This agrees with the smaller spread in $^{14}\text{a}_{\text{org,N}}$ for the RH-diluted series. The $\sigma[^{14}\text{a}_{\text{org,N}}]$ values and the spread are the largest for the series of VH diluted with S2 (not shown). Similar phenomena are found for the other 3 sample series.

The $\sigma[^{14}\text{a}_{\text{org,N}}]$ values of 75% of the samples differ for the 3 procedures, in that they are larger for procedure C at some of the higher x values. This is due to the 2nd term in (13), which increases rapidly with x , whereas the 2nd term in (12) does not. Because of these terms, it is worthwhile to keep $\sigma[\delta^{13}\text{C}_{\text{tot}}]$ as small as possible. Therefore, we calculate $\delta^{13}\text{C}_{\text{tot}}$ as the mean of 8 block averages weighted by the total ^{14}C counts for each block. The block average is the mean of 10 measurements at one and the same position on the target surface and the target surface is measured at 8 different positions. With this weighted mean, we reduced $\sigma[\delta^{13}\text{C}_{\text{tot}}]$ by an average factor of 2.8.

To study our approximation for $\sigma[^{14}\text{a}_{\text{org,N}}]$ quantitatively, we plotted the histogram of $(^{14}\text{a}_{\text{org,N}} - ^{14}\text{a}_{\text{N}})/\sigma[^{14}\text{a}_{\text{org,N}}]$ for the 6 sample series. That is, the deviation of the individual sample triplicate and measurement duplicate activities from their known values, relative to their calculated standard deviations. If our approximation for $\sigma[^{14}\text{a}_{\text{org,N}}]$ agrees with the spread in the experimental results, the histograms will show a normal distribution with a mean value ≈ 0 and a standard deviation ≈ 1 . Figures 7a and b show these histograms for the VH series diluted with C5 and RH according to procedures B and C, respectively. The histogram for procedure A is similar to B. In general, the graphs resemble a normal distribution with the mean values equal to -0.2 and 0.5 . For the 4 sample series that are not shown, the mean was in between these values. Next to that, the standard deviation of the distribu-

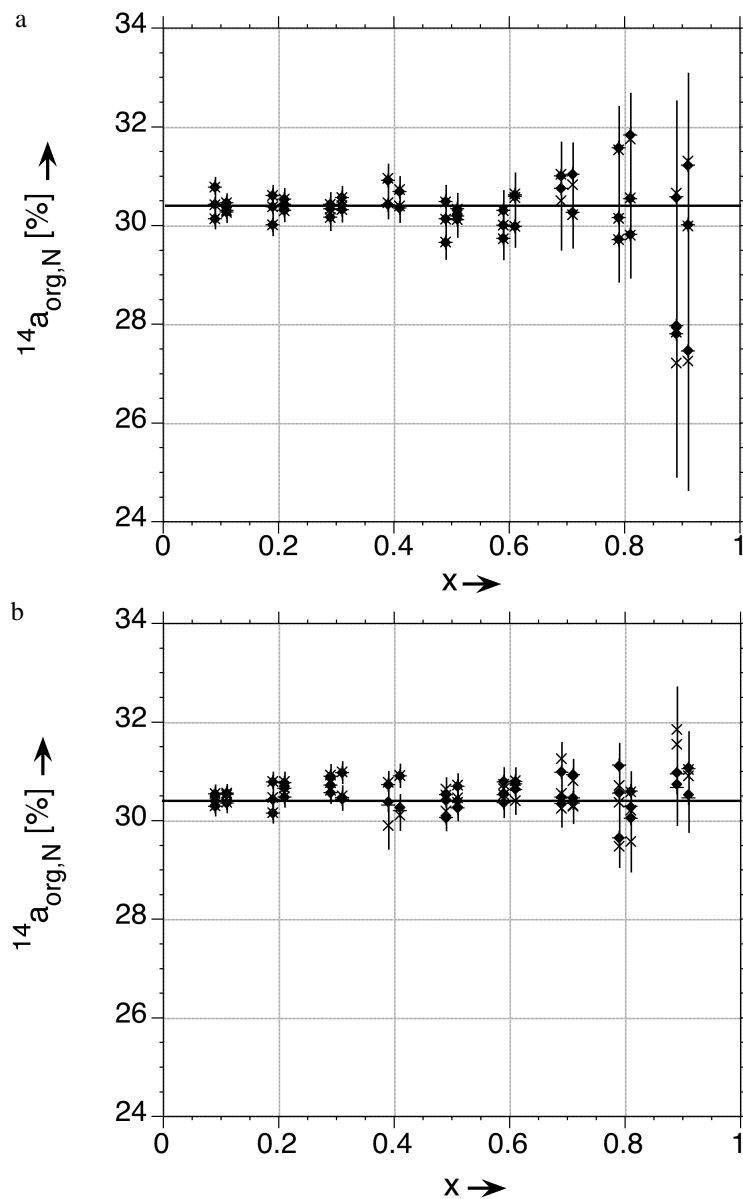


Figure 6 Calculated results for 2 of the 3 series of VH samples diluted to 2 mg C. Normalized activity of the original samples ($^{14}a_{\text{org,N}}$) as a function of x , a) for the series diluted with C5 and b) for the series diluted with RH. Notice that the measurement duplicates (both in triplicate) are displayed just left and right of their x values. The calculated results according to procedures A, B, and C are shown as \diamond , $+$, and \times , respectively.

tions is in between 0.7 (for C7 diluted with RH) and 1.1 (for VH diluted with RH). Therefore, the mean corresponds approximately to zero and the standard deviation is nearly equal to 1. This shows that our calculation of the standard deviation $\sigma[^{14}a_{\text{org,N}}]$ is reliable.

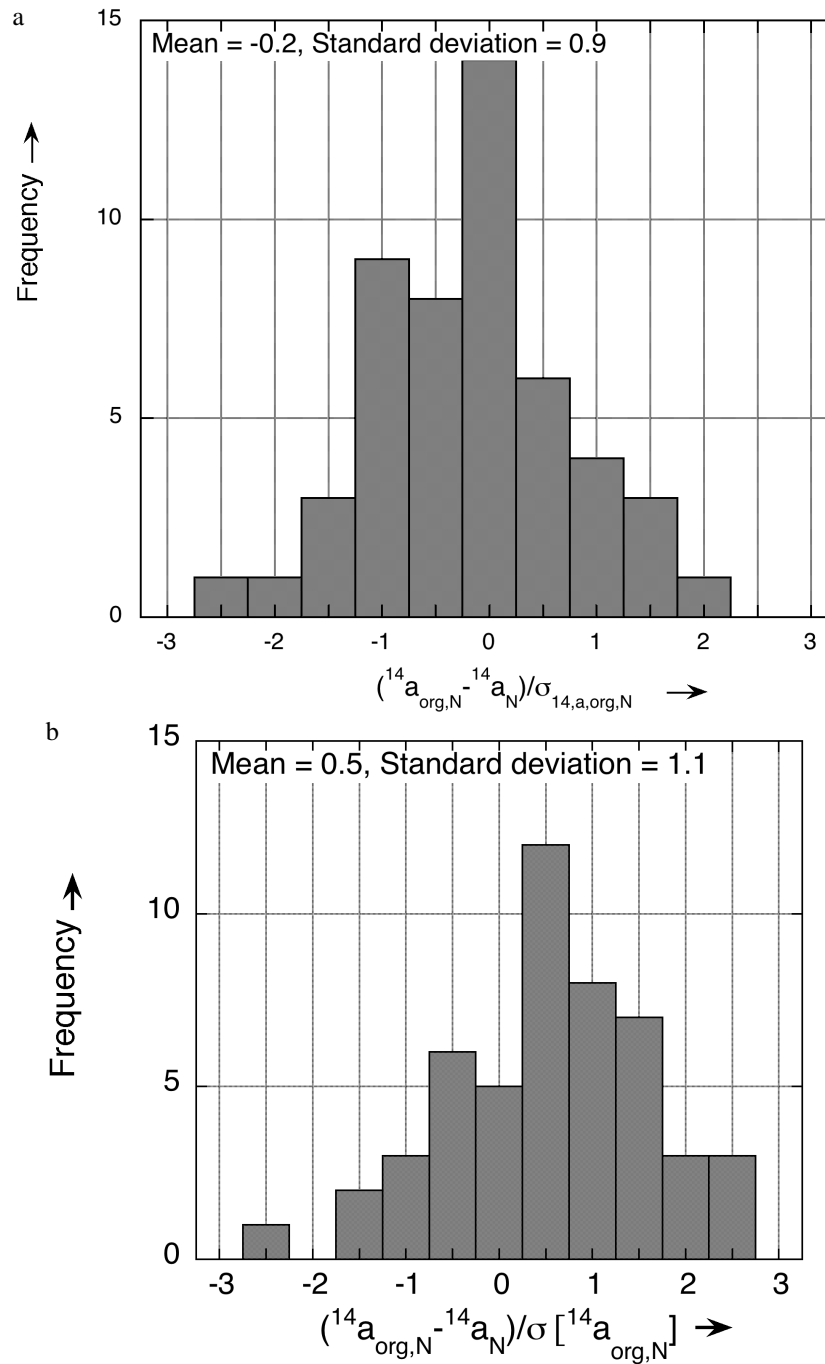


Figure 7 Histograms of $(^{14}\text{a}_{\text{org,N}} - ^{14}\text{a}_{\text{N}}) / \sigma [^{14}\text{a}_{\text{org,N}}]$ found for the sample triplicates and measurement duplicates of the VH samples diluted to 2 mg C. a) For samples diluted with C5, according to procedure B. b) For samples diluted with RH, according to procedure C. The histograms found according to procedure A are similar to those found from B. In general, the graphs resemble a normal distribution. The mean of the distributions corresponds approximately to zero and the standard deviation is close to the expected value of 1.

Small Samples Diluted to 200 µg C

The previous sample series show that the spread in the results agrees with the calculated standard deviations for samples diluted to 2 mg C. The value is mainly determined by the ratio between the diluent gas and total sample mass (x). For the next experiment, we used a more realistic series of 40 small samples. We tested the reduction reaction for a variety of sample sizes in our graphitization system, which has been designed for normal-sized samples (4.1 ± 0.4 mL). It showed that we need at least around 200 µg C of CO₂ to guarantee a high success rate for the sample analyses. To check our approximation of the standard deviation and our error values for this sample size, we also performed a dilution experiment with small samples. Our calculation study showed that a ¹⁴C-free diluent gas results in a higher precision. Therefore, we used HL to dilute the small samples to 200 µg C. The non-normalized activity of the total sample (¹⁴a_{tot}) was measured by AMS. On average, the ¹³C current in the accelerator was around 45% lower than for the 2-mg C samples. For 3 samples, we considered the ¹³C current to be too small (below 3×10^{-8} A). We rejected the results for these samples because they might not be reliable, even though we do find accurate results for some.

Figure 8a shows that ¹⁴a_{tot} decreases linearly with x for the C7 samples, as it should because the dilution is with ¹⁴C-free HL. The arrows point out 2 values for ¹⁴a_{tot} that are relatively low. So far, it is unclear what caused these low values. For one of them, the ¹³C current was rather low (6×10^{-8} A) but not so small to become unacceptable. The decrease in ¹⁴a_{tot} causes the standard deviation in the measured activity $\sigma[^{14}\text{a}_{\text{tot}}]$ to decrease in absolute terms with x as well (see Figure 8b). Notice that the spread in $\sigma[^{14}\text{a}_{\text{tot}}]$ values is relatively large for the 200-µg C samples. The values depend strongly on the ¹³C current: they appear to increase linearly with decreasing ¹³C current. Much to our surprise, we do not find a correlation between the ¹³C current and the sample mass for these samples. Presumably, this is because of variability in graphite and/or target surface quality.

We calculated the normalized activity (¹⁴a_{org,N}) for the remaining 37 original samples using procedures A and C, and for 27 of them also using procedure B. In general, the results agree very well with the ¹⁴C activity of C7 in Table 3 (see Figure 9a). The 2 samples with a relatively low value for ¹⁴a_{tot} that we pointed out in Figure 8a, however, resulted in 2 outliers for ¹⁴a_{org,N}. One of them (¹⁴a_N = $46.0 \pm 0.7\%$) is clearly visible in Figure 9a at $x = 0.52$. The other (¹⁴a_N = $33 \pm 3\%$) at $x = 0.94$ lies even below the range of the figure. It is quite remarkable that these outliers have a too-low ¹⁴C activity. We would have expected eventual outliers with too-high ¹⁴C activity, since the samples themselves have a relatively low activity due to the dilution with ¹⁴C-free HL gas. In an attempt to explain the outliers, we compared the x values that we found from the pressure readings to those that we found from the IRMS-measured values for $\delta^{13}\text{C}_{\text{org}}$, $\delta^{13}\text{C}_{\text{dil}}$, and $\delta^{13}\text{C}_{\text{tot}}$. Based on these, we find for x :

$$x = \frac{\delta^{13}\text{C}_{\text{tot, IRMS}} - \delta^{13}\text{C}_{\text{org, IRMS}}}{\delta^{13}\text{C}_{\text{dil, IRMS}} - \delta^{13}\text{C}_{\text{org, IRMS}}} \quad (18)$$

The measured and calculated x values agree for the 27 samples analyzed according to procedure B, including the outlier at $x = 0.94$. Therefore, the relatively low ¹⁴a_{tot} measured by the AMS system suggests accidental mixing with ¹⁴C-free material in the graphitization system. But so far, the cause of these outliers is not known.

The standard deviation in the normalized activity of the original samples ($\sigma[^{14}\text{a}_{\text{org,N}}]$) was approximated with (11) and either (12) or (13), depending on the procedure. The $\sigma[^{14}\text{a}_{\text{org,N}}]$ values, shown as a function of x in Figure 9b, are higher than those for the C7 sample series that we diluted to 2 mg C with RH (not shown). Except for the total sample size, the experiments are similar: HL and

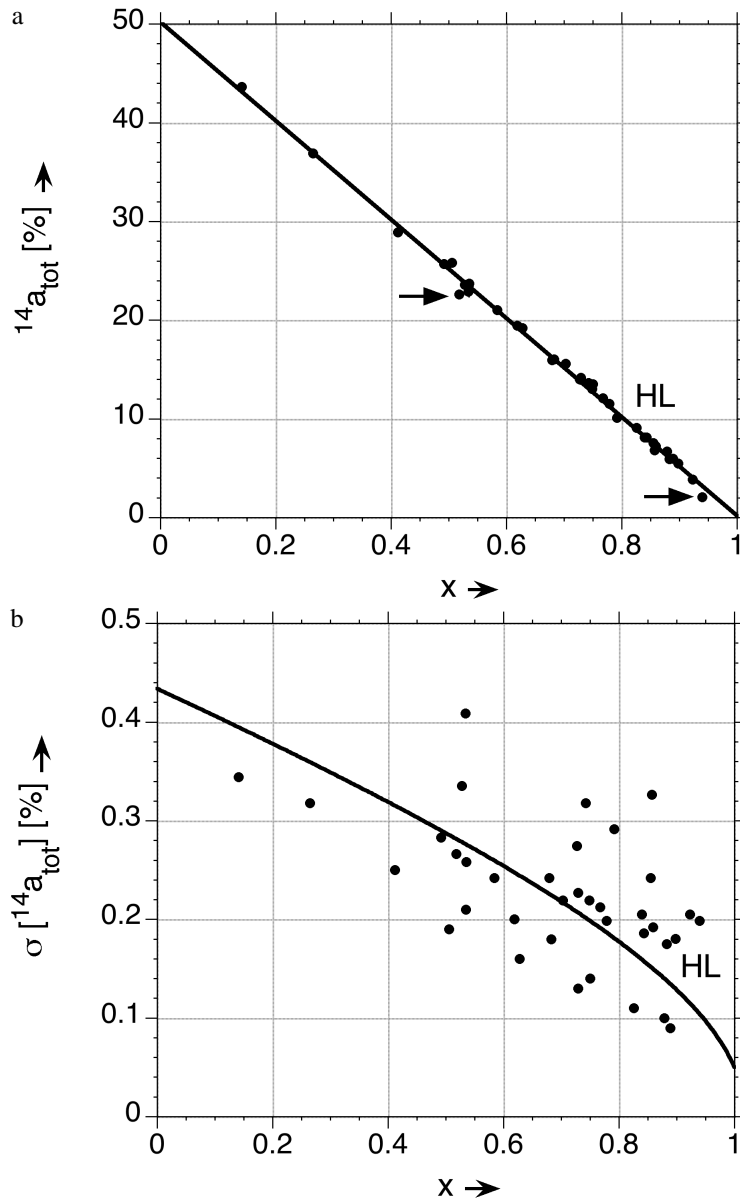


Figure 8 Measurement results for the series of C7 samples diluted to 200 μg C. a) Measured activity (non-normalized) of the total sample ($^{14}\text{a}_{\text{tot}}$) as a function of x . The standard deviations are not visible because they are smaller than the symbol size. The arrows point out 2 outliers. b) Standard deviation in the measured activity of the total sample $\sigma[^{14}\text{a}_{\text{tot}}]$ as a function of x .

RH are both ^{14}C free and we know from our calculation study that $\sigma[^{14}\text{a}_{\text{org,N}}]$ does not depend on the $\delta^{13}\text{C}$ values. The larger errors for the 200-μg C samples are mainly due to higher $\sigma[^{14}\text{a}_{\text{tot}}]$ values.

Above that, the standard deviation in the $\delta^{13}\text{C}$ value measured by AMS ($\sigma[\delta^{13}\text{C}_{\text{tot}}]$) is also relatively high for the 200-μg C samples. This causes $\sigma[^{14}\text{a}_{\text{org,N}}]$ to depend significantly on the procedure that

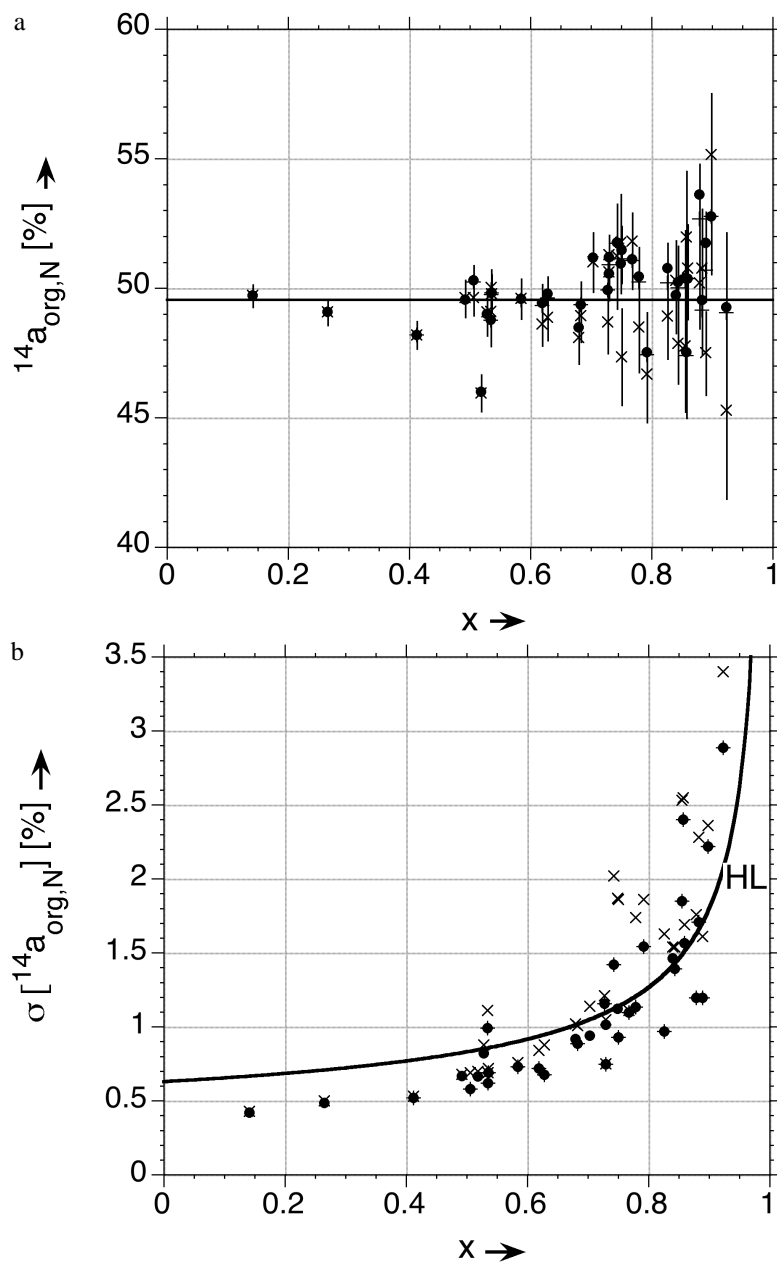


Figure 9 Calculated results for the series of C7 samples diluted to 200 μg C. a) Normalized activity of the original samples ($^{14}a_{\text{org},N}$) as a function of x . b) Standard deviation in the normalized activity of the original samples $\sigma[^{14}a_{\text{org},N}]$ as a function of x . Calculated results found according to procedures A, B, and C are represented by \blacklozenge , $+$, and \times , respectively.

is used. For 25 out of the 37 samples, the difference between the 2nd term in (12) and (13) causes $\sigma[^{14}a_{\text{org},N}]$ according to procedure C to be significantly higher than $\sigma[^{14}a_{\text{org},N}]$ according to procedures A and B.

The $\sigma[^{14}\text{a}_{\text{org},\text{N}}]$ values increase rapidly with x , because the 1st term in (11) is the dominant term. This appears to correspond to the increase in the spread in $^{14}\text{a}_{\text{org},\text{N}}$ with x . The phenomenon appears to be stronger for $^{14}\text{a}_{\text{org},\text{N}}$ found using procedure C, which would agree with the higher $\sigma[^{14}\text{a}_{\text{org},\text{N}}]$ values found according to this procedure.

To study our approximation for $\sigma[^{14}\text{a}_{\text{org},\text{N}}]$ quantitatively, we plotted the histogram of $(^{14}\text{a}_{\text{org},\text{N}} - ^{14}\text{a}_{\text{N}}) / \sigma[^{14}\text{a}_{\text{org},\text{N}}]$ for the 200- μg C samples. Figures 10a,b,c show the histograms for the C7 samples diluted with HL according to procedures A, B, and C, respectively.

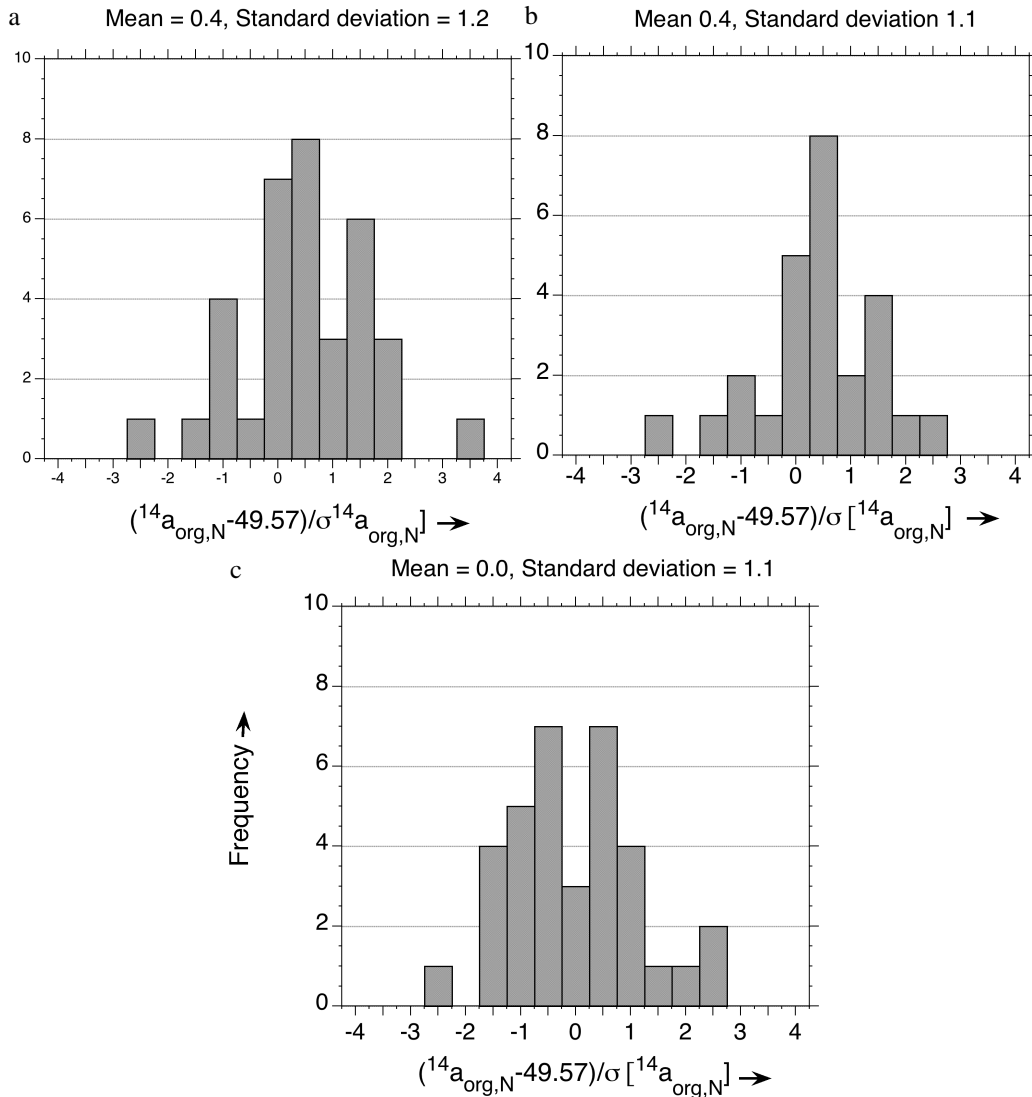


Figure 10 Histograms of $(^{14}\text{a}_{\text{org},\text{N}} - 49.57) / \sigma[^{14}\text{a}_{\text{org},\text{N}}]$ found for C7 samples diluted to 200 μg C after omitting 2 outliers: a) according to procedure A; b) procedure B; and c) procedure C. In general, the graphs resemble a normal distribution. The mean of the distributions corresponds approximately to zero and the standard deviation is close to 1.

In general, we can recognize a normal distribution in the graphs. After omitting the 2 outliers, the mean value = 0.4 (procedures A and B) and 0.0 (procedure C), and the standard deviation is 1.2 (pro-

cedure A) or 1.1 (procedures B and C). When we include the outliers, the mean is in between -0.4 and 0.1 and the standard deviation varies from 1.5 to 1.9 . Apart from the outliers, with values that suggest accidental mixing with ^{14}C -free material in the graphitization system, the mean corresponds again approximately to zero and the standard deviation ratio is nearly equal to 1. This is a firm indication that our calculation of $\sigma[^{14}a_{\text{org},N}]$ is also a good approximation for the standard deviation for $200\text{-}\mu\text{g C}$ samples. The extra handling and IRMS measurement of the total sample (procedure B) did not cause any significant contamination for the $200\text{-}\mu\text{g C}$ samples.

The results that we found according to the different procedures agree for each of the samples. The $^{14}a_{\text{org},N}$ values are approximately equal for procedures A and B and within 1 standard deviation for 90% of the samples for procedure C.

We obtained accurate results for approximately 90% of the small samples ($<150\ \mu\text{g C}$) by using sample dilution. A higher success rate (up to 95%) seems feasible because the 2 outliers appear to have been caused by a mistake during preparation or handling of the sample, and we rejected 3 samples because we considered the ^{13}C current to be too small. The total sample will have a relatively low ^{14}C activity because we use a ^{14}C -free diluent gas. Because of that, the sample is susceptible to contamination with modern material. Although our experiment did not suffer from any significant contamination, great care needs to be taken in using a proper background correction.

200- $\mu\text{g C}$ Backgrounds

The standard deviation in the normalized activity of the original sample $\sigma[^{14}a_{\text{org},N}]$ is found from (11) and either (12) or (13) depending on the procedure. The 1st term on the right-hand side of (11) dominates $\sigma[^{14}a_{\text{org},N}]$. It comprises $\sigma[^{14}a_{\text{tot}}]$, which consists of 3 terms: the spread in the HOxII standards in the batch, the standard deviation in the measured $^{14}\text{C}/^{12}\text{C}$ ratio of the sample (Poisson error), and the spread in the RH backgrounds in the batch. Because we use a ^{14}C -free diluent gas, the total sample will have a relatively low ^{14}C activity. This makes the spread in the RH background activities an important error source. Moreover, it determines the lowest possible activity that we can obtain for an original sample that is analyzed with sample dilution.

The 2-mg C and $200\text{-}\mu\text{g C}$ samples were measured in different batches with RH backgrounds and HOxII standards of the same size. Figure 11 shows the normalized activity for RH background samples of $200\ \mu\text{g C}$ from 5 different batches. The results are corrected for the mean RH background of their batches. The spread in the background values is larger than suggested by their standard deviations (0.11% vs. 0.07%). Therefore, we use the observed standard deviation as an indication for the lowest significant activity that we can still measure.

Because the 1st term in (11) dominates the standard deviation in the normalized activity of the original sample, the approximation $\sigma[^{14}a_{\text{tot}}]/(1-x)$ gives a reasonable estimate for $\sigma[^{14}a_{\text{org},N}]$. Therefore, the minimum value that we can obtain for the normalized activity of the original sample is approximated by:

$$^{14}a_{\text{org},N} = \frac{2 \cdot 0.11\%}{1-x} \quad (19)$$

The observed standard deviation in the background values is multiplied by a factor 2 in order to reach 95% reliability. This also prevents, for all practical purposes, the occurrence of negative activities (Olsson 1989).

In the present experimental setup, this results in a decrease of the age limit of the original sample from 48,000 to 31,000 ^{14}C yr BP as the x value increases from 0.1 to 0.9.

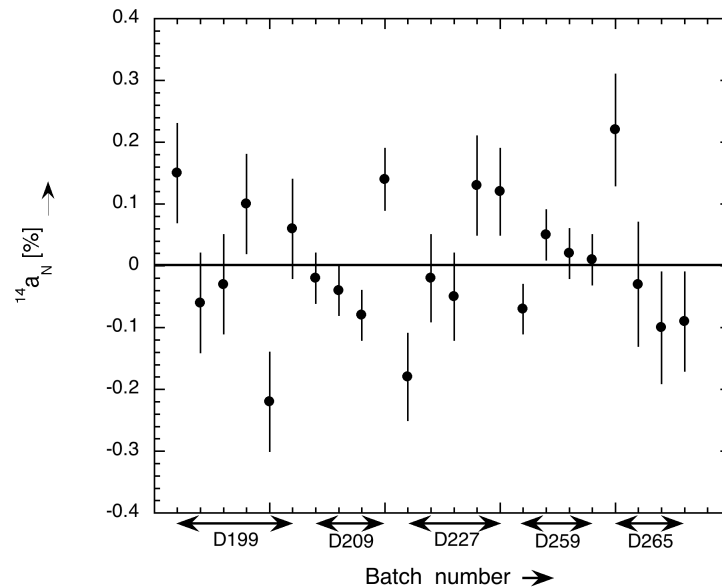


Figure 11 Normalized activity for RH backgrounds ($200 \mu\text{g C}$) from 5 different batches. The results are corrected for the batch mean RH background. The spread in the backgrounds is about 0.11%.

Ice-Core Samples

Our investigation proves that we can rely on sample dilution to analyze small ice-core samples. Therefore, we used sample dilution to find the ^{14}C activity of CO_2 samples taken from the EDML ice core drilled in Dronning Maud Land (DML) as part of the European Project for Ice Coring in Antarctica (EPICA). ^{14}C dating of the CO_2 contained in air bubbles in ice cores is a fully independent way of dating the vertical ice profile (van de Wal et al. 1994; de Jong et al. 2004). For this specific project, the CO_2 that was extracted from the air bubbles of 18 precious ice-core samples contained approximately $35 \mu\text{g C}$. In the laboratory of the Institute for Marine and Atmospheric Research of the University of Utrecht (IMAU), CO_2 was extracted from the ice and then diluted with ^{14}C -free HL to $200 \mu\text{g C}$ on average. Each of the extracted CO_2 samples was accompanied by a HL background sample, which was formed by filling up the ice-milling equipment with ^{14}C -free HL prior to extraction. After graphitization and measurement at the Groningen AMS laboratory, the total CO_2 samples and HL backgrounds were first corrected for the batch mean RH value. This value represents the Groningen AMS laboratory handling and analysis background. Then, the normalized activity of the total CO_2 samples was corrected for the mean value of the corrected HL backgrounds ($0.33 \pm 0.17\%$).

All ice-core samples were analyzed successfully using procedure C. After we managed to remove the vapor of drilling fluid properly from the CO_2 samples, we were able to measure the true $\delta^{13}\text{C}$ value for some of the total samples ($\delta^{13}\text{C}_{\text{tot,IRMS}}$). (Traces of drilling fluid interfere with the isotope masses 45 and 46 of CO_2 in the IRMS, and can lead to large deviations.) Therefore, we also found $^{14}\text{a}_{\text{org,N}}$ according to procedure B for 6 of the samples. The results for the ice-core samples are shown as a function of their depth in the EDML ice core in Figure 12 and the values are shown in Table 4. Clearly, $^{14}\text{a}_{\text{org,N}}$ decreases significantly with increasing depth, which corresponds to increasing age of the ice-core sample. It ranges from 109% down to not significantly different from the background value. The ice-core samples show a smooth trend with depth, except at 782–783 m. This CO_2 sam-

ple was contaminated with modern air due to a leakage in the ice-milling equipment at the time of extraction. The measured deviation indeed agrees with our estimate of the amount of modern air that has leaked into the sample.

Table 4 Results for the CO₂ samples from the EDML ice core. GrA-28539 suffered from a leakage in the ice-milling equipment at the time of extraction.

GrA-	Depth in EDML core (m)	x	$^{14}a_{\text{tot}}$ (%)	$^{14}a_{\text{org,N}}$ (%) calculated by procedure B	$^{14}a_{\text{org,N}}$ (%) calculated by procedure C
28528	118–119	0.83	19.08 ± 0.23	105.2 ± 1.8	104.9 ± 2.1
28534	143–144	0.82	18.22 ± 0.25	99.9 ± 1.8	106.1 ± 2.4
26207	165–166	0.82	19.19 ± 0.32		109.0 ± 2.5
26699	266–267	0.81	19.55 ± 0.26		97.0 ± 2.0
26212	366–367	0.81	16.01 ± 0.35		83.7 ± 2.2
26704	465–466	0.82	14.69 ± 0.23		78.7 ± 1.6
26217	562–563	0.85	10.71 ± 0.28		70.6 ± 2.2
26710	665–666	0.80	11.62 ± 0.22		55.6 ± 1.4
26221	766–767	0.83	8.69 ± 0.28		49.0 ± 1.9
28539	782–783	0.80	14.24 ± 0.22	68.3 ± 1.3	70.0 ± 1.5
28869	841–842	0.85	4.25 ± 0.17		27.2 ± 1.3
26722	866–867	0.86	3.91 ± 0.19		26.6 ± 1.4
26231	970–971	0.87	2.46 ± 0.26		18.5 ± 2.0
27393	1066–1067	0.86	2.13 ± 0.20		13.7 ± 1.4
26236	1165–1166	0.84	1.41 ± 0.26		8.6 ± 1.6
27386	1266–1267	0.87	0.75 ± 0.19	5.2 ± 1.4	5.6 ± 1.5
27387	1365–1366	0.89	0.24 ± 0.19	1.7 ± 1.4	2.2 ± 1.8
27376	1469–1470	0.86	0.07 ± 0.19	0.5 ± 1.3	0.5 ± 1.4

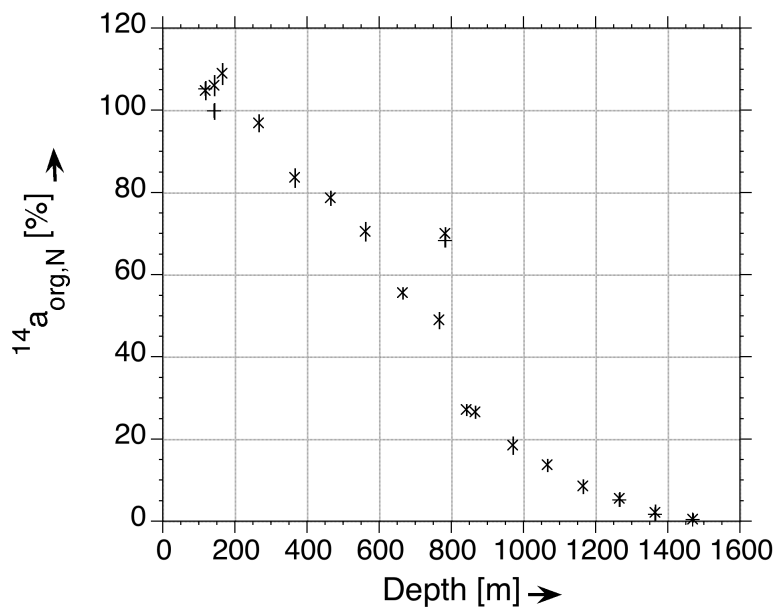


Figure 12 Calculated results for the EDML ice-core samples diluted to 200 µg C. a) Normalized activity of the original samples ($^{14}a_{\text{org,N}}$) as a function of the ice sample depth. Calculated results found according to procedures B and C are shown as + and *, respectively.

The results that were calculated according to procedures B and C are in very good agreement. Only at depths 143–144 m, the value for $^{14}\text{a}_{\text{org,N}}$ according to procedure B is significantly lower than from procedure C. The difference is due to an exceptionally large difference between the actual and the assumed fractionation factor used for this sample in procedures B and C, respectively. Presumably, the $\delta^{13}\text{C}_{\text{tot,IRMS}}$ still suffered from contamination with drilling fluid vapor.

From $^{14}\text{a}_{\text{org,N}}$ found according to procedure C, we calculated the ^{14}C age of the original sample using (9). Table 4 shows the results together with the standard deviation in the ^{14}C age. It was found from (14) for all the samples, except the 3 oldest for which we used (15). We refer to van de Wal et al. (2007) for interpretation of the results and further details.

CONCLUSIONS

We investigated the use of sample dilution for AMS ^{14}C analysis of small samples down to 30 $\mu\text{g C}$. Through our extensive calculation study and dilution experiment, we reached the following answers to our research questions:

1. We determine the normalized activity of the original (small) sample by selecting 1 out of 3 procedures. The choice depends on whether we know: the actual $\delta^{13}\text{C}$ value of the original sample, the actual $\delta^{13}\text{C}$ value of the total (diluted) sample, or the fractionation by the AMS system. The first 2 procedures are normally preferred over the last one. Therefore, the proper $\delta^{13}\text{C}$ values should be measured by stable isotope ratio mass spectrometry (IRMS). If this is not possible, the activity is found by assuming that the AMS-induced fractionation factor for the sample is the same as for the standards in the batch.
2. The uncertainty in the normalized activity of the original sample is determined by 5 error sources. The error in the ^{14}C activity measured by the AMS system for the total diluted sample is the dominant one. The others are the error in the diluent gas activity, the masses of the original sample and diluent gas, and the $\delta^{13}\text{C}$ value measured by the AMS system for the total sample.
3. The best choice for the diluent gas to achieve the highest precision is a ^{14}C -free CO_2 gas. The choice for the $\delta^{13}\text{C}$ value of the diluent gas is not important. The optimum result in terms of precision is achieved when the added amount of diluent gas is as small as possible.
4. The smallest sample size that still yields accurate ^{14}C activities in our current setup is currently around 200 $\mu\text{g C}$. We need to dilute the original (small) sample to at least this amount for successful handling and analysis of >90% of the samples.
5. The age limit for a small sample using sample dilution ranges from 48,000 to 31,000 BP when the ratio between the diluent gas and total sample mass increases from 0.1 to 0.9.

Our investigation proved that sample dilution is a reliable means to find the ^{14}C activity of precious small samples (<150 $\mu\text{g C}$) that are irreplaceable. By using sample dilution, we were able to successfully measure the ^{14}C activity of the CO_2 that was extracted from the air bubbles of 18 Antarctic ice-core samples. Each of the original CO_2 samples, which contained approximately 35 $\mu\text{g C}$, was diluted to a total sample size of at least around 200 $\mu\text{g C}$. With our present experimental setup, this resulted in $\sigma[^{14}\text{a}_{\text{org,N}}] = 1.8\%$ for a modern sample. Because the standard deviation in the distribution of the 200- $\mu\text{g C}$ backgrounds is $\sigma[^{14}\text{a}_{\text{tot}}] = 0.11\%$, an upper age limit of 36,000 BP should be feasible for an original sample size of only 35 $\mu\text{g C}$.

What remains is the price that we pay regarding precision. Therefore, our future research will focus on achieving a higher precision. We are going to use smaller graphitization reactors. This will increase our graphitization yield for samples of 200 $\mu\text{g C}$, which is currently only ~70%. It will also enable us to graphitize smaller sample amounts successfully and thus use a smaller dilution factor.

In the future, we will use an extremely porous iron pellet as a catalyst instead of iron powder. Using an iron pellet with a diameter equal to the drilled hole in the target holder results in a more homogeneous target surface; hence, it will increase the sputter yield and make it less variable. Initial tests show that this new approach for the AMS ^{14}C analysis of small samples is a promising development. It will allow us to reduce the total sample size even further, since the required amount of carbon to guarantee an accurate analysis will be smaller. Because the error in the activity $\sigma[^{14}\text{a}_{\text{org,N}}]$ increases rapidly with the dilution factor x , this will increase the precision to a high extent. Moreover, it is also expected to greatly enhance the success rate of samples down to ultra-microscale size, defined as 5–25 $\mu\text{g C}$.

REFERENCES

- Aerts-Bijma AT, Meijer HAJ, van der Plicht J. 1997. AMS sample handling in Groningen. *Nuclear Instruments and Methods in Physics Research B* 123(1–4): 221–5.
- Alderliesten C, van der Borg K, de Jong AFM. 1998. Contamination and fractionation effects in AMS-measured $^{14}\text{C}/^{12}\text{C}$ and $^{13}\text{C}/^{12}\text{C}$ ratios of small samples. *Radiocarbon* 40(1):215–21.
- Brown TA, Southon JR. 1997. Corrections for contamination background in AMS ^{14}C measurements. *Nuclear Instruments and Methods in Physics Research B* 123(1–4):208–13.
- Bruins HJ, van der Plicht J, Mazar A. 2003. ^{14}C dates from Tel Rehov: Iron-Age chronology, pharaohs, and Hebrew kings. *Science* 300(5617):315–8.
- de Jong AFM, Alderliesten C, van der Borg K, van der Veen C, van de Wal RSW. 2004. Radiocarbon analysis of the EPICA Dome C ice core: no in situ ^{14}C from the firm observed. *Nuclear Instruments and Methods in Physics Research B* 223–224:516–20.
- Gott dang A, Mous DJW, van der Plicht J. 1995. The HVEE ^{14}C system at Groningen. *Radiocarbon* 37(2): 649–56.
- Hua Q, Zoppi U, Williams AA, Smith AM. 2004. Small-mass AMS radiocarbon analysis at ANTARES. *Nuclear Instruments and Methods in Physics Research B* 223–224:284–92.
- Klinedinst DB, McNichol AP, Currie LA, Schneider RJ, Klouda GA, von Reden KF, Verkouteren RM, Jones GA. 1994. Comparative study of Fe-C bead and graphite target performance with the National Ocean Science AMS (NOSAMS) facility recombinator ion source. *Nuclear Instruments and Methods in Physics Research B* 92(1–4):166–71.
- Le Clercq M, van der Plicht J, Gröning M. 1998. New ^{14}C reference materials with activities of 15 and 50 pMC. *Radiocarbon* 40(1):295–7.
- Meijer HAJ, Pertuisot MH, van der Plicht J. 2006. High-accuracy ^{14}C measurements for atmospheric CO_2 samples by AMS. *Radiocarbon* 48(3):355–72.
- Mook WG, Streurman HJ. 1983. Physical and chemical aspects of radiocarbon dating. *PACT* 8:31–55.
- Mook WG, van der Plicht J. 1999. Reporting ^{14}C activities and concentrations. *Radiocarbon* 41(3):227–39.
- Olsson IU. 1989. The ^{14}C method—its possibilities and some pitfalls. *PACT* 24:161–77.
- Santos GM, Southon JR, Griffin S, Beaupre SR, Druffel ERM. 2007. Ultra small-mass AMS ^{14}C sample preparation and analyses at KCCAMS/UCI Facility. *Nuclear Instruments and Methods in Physics Research B* 259(1):293–302.
- Schneider RJ, Kim S-W, von Reden KF, Hayes JM, Wills JSC, Griffin VS, Sessions AL, Sylva S. 2004. A gas ion source for continuous-flow AMS. *Nuclear Instruments and Methods in Physics Research B* 223–224: 149–54.
- Scott EM, Bryant C, Cook GT, Naysmith P. 2003. Is there a Fifth International Radiocarbon Intercomparison (VIRI)? *Radiocarbon* 45(3):493–5.
- Uhl T, Kretschmer W, Luppold W, Scharf A. 2005. AMS measurements from microgram to milligram. *Nuclear Instruments and Methods in Physics Research B* 240(1–2):474–7.
- van de Wal RSW, van Roijen JJ, Raynaud D, van der Borg K, de Jong AFM, Oerlemans J, Lipenkov V, Huybrechts P. 1994. From $^{14}\text{C}/^{12}\text{C}$ measurements towards radiocarbon dating of ice. *Tellus B* 46(2):94–102.
- van de Wal RSW, Meijer HAJ, de Rooij M, van der Veen C. 2007. Radiocarbon analyses along the EDML ice core in Antarctica. *Tellus B* 59(1):157–65.
- van der Plicht J, Wijma S, Aerts AT, Pertuisot MH, Meijer HAJ. 2000. Status report: the Groningen AMS facility. *Nuclear Instruments and Methods in Physics Research B* 172(1–4):58–65.
- van der Plicht J, van der Sanden WAB, Aerts AT, Streurman HJ. 2004. Dating bog bodies by means of ^{14}C -AMS. *Journal of Archaeological Science* 31(1):471–91.
- van Geel B, van der Plicht J, Kilian MR, Klaver ER, Koutenberg JHM, Renssen H, Reynaud-Farrera I, Waterbolk HT. 1998. The sharp rise of $\Delta^{14}\text{C}$ ca. 800 cal BC: possible causes, related climatic teleconnections and the impact on human environments. *Radiocarbon* 40(1):535–50.
- von Reden KF, McNichol AP, Pearson A, Schneider RJ. 1998. ^{14}C AMS measurements of <100 μg samples with a high-current system. *Radiocarbon* 40(1):247–53.